



Discover Generics

Cost-Effective CT & MRI Contrast Agents



FRESENIUS
KABI

WATCH VIDEO

AJNR

This information is current as
of June 6, 2025.

Diagnostic Performance of High-Resolution Vessel Wall MR Imaging Combined with TOF-MRA in the Follow-up of Intracranial Vertebrobasilar Dissecting Aneurysms after Reconstructive Endovascular Treatment

S. Tan, X. Zhou, X. Xu, Y. Lu, X. Zeng, Q. Wu and Y.
Wang

AJNR Am J Neuroradiol 2023, 44 (4) 453-459

doi: <https://doi.org/10.3174/ajnr.A7838>

<http://www.ajnr.org/content/44/4/453>

Diagnostic Performance of High-Resolution Vessel Wall MR Imaging Combined with TOF-MRA in the Follow-up of Intracranial Vertebrobasilar Dissecting Aneurysms after Reconstructive Endovascular Treatment

 S. Tan,  X. Zhou,  X. Xu,  Y. Lu,  X. Zeng,  Q. Wu, and  Y. Wang



ABSTRACT

BACKGROUND AND PURPOSE: Few studies have reported the utility of high-resolution vessel wall MR imaging in the follow-up of endovascularly treated vertebrobasilar dissecting aneurysms. This study aimed to evaluate the diagnostic performance of high-resolution vessel wall MR imaging combined with TOF-MRA in the follow-up of intracranial vertebrobasilar dissecting aneurysms after reconstructive endovascular treatment.

MATERIALS AND METHODS: Patients with intracranial vertebrobasilar dissecting aneurysms with reconstructive endovascular treatment and followed up with TOF-MRA, high-resolution vessel wall MR imaging, and DSA were included. With DSA as the criterion standard, the diagnostic performance of TOF-MRA, high-resolution vessel wall MR imaging, and high-resolution vessel wall MR imaging combined with TOF-MRA in the evaluation of aneurysm occlusion status and parent artery patency was assessed. Visualization of the stented artery on TOF-MRA and high-resolution vessel wall MR imaging was rated on a 5-point scale.

RESULTS: Twenty-seven patients with 29 aneurysms were included. The sensitivity, specificity, positive predictive value, and negative predictive value of TOF-MRA, high-resolution vessel wall MR imaging, and high-resolution vessel wall MR imaging combined with TOF-MRA for diagnosing aneurysm remnants were 80.0%, 100.0%, 100.0%, and 82.4%; 53.3%, 100.0%, 100.0%, and 66.7%; and 93.3%, 100.0%, 100.0%, and 93.3%, respectively. For the visualization of the stented artery, the mean score of high-resolution vessel wall MR imaging was significantly higher than that of TOF-MRA (4.88 [SD, 0.32] versus 2.53 [SD, 1.25], $P < .001$). In the evaluation of parent artery patency (normal or pathologic), whereas TOF-MRA had a sensitivity, specificity, positive predictive value, and negative predictive value of 100.0%, 8.0%, 14.8%, and 100.0%, respectively, high-resolution vessel wall MR imaging was completely consistent with the DSA.

CONCLUSIONS: High-resolution vessel wall MR imaging combined with TOF-MRA at 3T showed good diagnostic performance in the follow-up of intracranial vertebrobasilar dissecting aneurysms after reconstructive endovascular treatment.

ABBREVIATIONS: EVT = endovascular treatment; HR-VW-MR imaging = high-resolution vessel wall MR imaging; IMH = intramural hematoma; SPACE = sampling perfection with application-optimized contrasts by using different flip angle evolutions; VBDA = vertebrobasilar dissecting aneurysm

Intracranial dissecting aneurysms are rare and are usually located at the vertebrobasilar artery. The treatment of intracranial vertebrobasilar dissecting aneurysms (VBDAs) is challenging and difficult. Compared with surgical treatment, endovascular treatment

(EVT) has less treatment-associated morbidity and mortality and has become the major treatment method for intracranial VBDAs.¹ However, for VBDAs treated with reconstructive EVT, imaging follow-up is imperative to detect recurrence in a timely manner.² DSA, the criterion standard for imaging follow-up, is invasive and has radiation exposure. Patients tend not to accept long-term repeat DSA follow-up examinations. Therefore, a noninvasive imaging technique is needed in clinical practice.

Received December 13, 2022; accepted after revision February 14, 2023.


From the Departments of Neurosurgery (S.T., Y.L., X. Zhou, Y.W.) and Radiology (X. Zeng, Q.W.), The First Affiliated Hospital of Nanchang University, Nanchang University, Nanchang, Jiangxi Province, China; Department of Neurosurgery (X.X.), The First People's Hospital of Zhaoqing City, Zhaoqing, Guangdong Province, China; and Department of Neurosurgery (Y.W.), Beijing Chaoyang Hospital, Capital Medical University, Beijing, China.

Yang Wang and Xiaobing Zhou contributed equally to this work.

Song Tan and Xiaobing Zhou would be designated as co-authors.

This study was founded by the National Natural Science Foundation of China (No. 8196070077), the Natural Science Foundation of Jiangxi Province (No. 20202BABL206053), and the National Key R&D program of China (No. 2016YFC1300802).

Please address correspondence to Yang Wang, MD, Department of Neurosurgery, Beijing Chaoyang Hospital, Capital Medical University, No. 8, South Gongti Rd, Chaoyang District, Beijing 100020, China; e-mail: wangyang7839@163.com

 Indicates open access to non-subscribers at www.ajnr.org

<http://dx.doi.org/10.3174/ajnr.A7838>

Table 1: Imaging parameters of MR imaging sequences

Parameters	TOF-MRA	3D T1-Weighted SPACE
TR (ms)	21	900
TE (ms)	3.43	16
Flip angle	18°	—
FOV (mm)	180 × 180	200 × 200
Matrix	320 × 320	384 × 384
No. of excitations	1	1
Section thickness (mm)	0.55	0.53
No. of slices	162	256
Echo-train length	—	293
Scanning time (min)	4:05	9:18

Note:—The en dash indicates not applicable.

Because of the severe artifacts arising from stents or coils, CTA is seldom used in the follow-up of endovascularly treated intracranial aneurysms. As a noninvasive imaging technique without radiation exposure, TOF-MRA has been widely used in the follow-up of these aneurysms.³ In VBDA, compared with saccular aneurysms, the injury of the arterial wall is more complex, and greater attention must be paid to the repair of the injured vessel wall during the follow-up period. Both DSA and MRA depict only geometric shapes of the arterial lumen by blood flow signals but cannot visualize the vessel wall. In contrast, high-resolution vessel wall MR imaging (HR-VW-MR imaging) can reveal the arterial lumen and wall simultaneously by suppressing the flow signals. In our center (First Affiliated Hospital of Nanchang University), HR-VW-MR imaging combined with TOF-MRA has been the most common follow-up imaging technique for intracranial VBDA. Multiple studies have reported the utility of HR-VW-MR imaging in the diagnosis of intracranial VBDA.⁴⁻⁷ However, few studies have reported the utility of HR-VW-MR imaging in the follow-up of endovascularly treated VBDA to date. In this study, we aimed to evaluate the diagnostic performance of HR-VW-MR imaging combined with TOF-MRA in the follow-up of intracranial VBDA treated with reconstructive EVT.

MATERIALS AND METHODS

Ethics Approval

This study was approved by the ethics committee of First Affiliated Hospital of Nanchang University (Nanchang, China, No. 2020047).

Patient Cohort

The local institutional review board (First Affiliated Hospital of Nanchang University) approved this study. Because the study was retrospective, the requirement for written informed consent was waived. Between January 2016 and December 2021, patients with intracranial VBDA treated with reconstructive EVT and followed up with HR-VW-MR imaging, TOF-MRA, and DSA in our center were included. If the interval between HR-VW-MR imaging and the DSA examination was >2 weeks, the patient was excluded. Patients' baseline and treatment information was acquired from the medical record system.

Image Acquisition

The MR imaging examination was performed on a 3T system (Magnetom Skyra; Siemens) with a 20-channel head and neck

united coil. A TOF-MRA was performed first. HR-VW-MR imaging included pre- and postcontrast 3D T1-weighted sampling perfection with application-optimized contrasts by using different flip angle evolutions (SPACE) sequences. Postcontrast images were obtained 5 minutes after venous injection of single-dose (0.1 mmol/kg) gadopentetate dimeglumine (Magnevist; Bayer HealthCare Pharmaceuticals) with the same parameters as for the precontrast T1-weighted images. The scanning range included the whole brain. The scan parameters are listed in Table 1.

With transfemoral catheterization, EVT and follow-up DSA were performed with the following angiographic systems: UNIQU FD20/15 (Philips Healthcare) or Axiom Artis dFA (Siemens).

Image Analysis

All images were reviewed blindly in random order by 2 interventional neuroradiologists with >10 years' experience. Only the locations of the treated aneurysms were provided to the reviewers. TOF-MRA and HR-VW-MR imaging were reviewed separately with an interval of 1 month. For TOF-MRA, both MIP images and source images were reviewed. For 3D T1 SPACE, MPRs were performed in the axial and oblique sagittal directions to visualize VBDA from different planes. The image quality of the stented artery on TOF-MRA and HR-VW-MR imaging was rated on the following 5-point scale:⁸ 1) not visible (the arterial structure was invisible, and strong artifacts were present); 2) poor (structures were slightly visible, and substantial artifacts or blurring was present); 3) acceptable (the diagnostic quality was acceptable, and moderate artifacts or blurring was present); 4) good (the images were of good quality, and minimal artifacts or blurring was present); or 5) excellent (the depiction was nearly equal to that of DSA). In cases of disagreement, the scores of the 2 reviewers were averaged. The patency of the parent artery was divided into 3 grades (normal, stenosis, or occlusion) or 2 grades on a simplified scale (normal or pathologic [stenosis or occlusion]). The aneurysm occlusion status was classified as complete or incomplete occlusion. Complete occlusion was defined by an absence of contrast agent in the aneurysmal sac observed on DSA, no flow signal in the aneurysmal sac on TOF-MRA, or no flow void in the aneurysmal sac on HR-VW-MR imaging. Otherwise, the aneurysm was considered incomplete occlusion. In cases of discrepancy, a consensus was reached between the reviewers by discussion.

After another month, the TOF-MRA and HR-VW-MR imaging findings were again reviewed together. After the diagnostic information from TOF-MRA and HR-VW-MR imaging was combined, the aneurysm occlusion status and parent artery patency were assessed. In cases of discrepancy, a consensus was reached by discussion.

DSA images were reviewed 1 month later by the same reviewers without knowledge of the MR imaging results. The evaluation included the aneurysm occlusion status and parent artery patency with the same classification standard used for the MR imaging examinations.

To investigate the vessel wall features of VBDA after procedures, the presence of an intimal flap, double lumen sign, or intramural hematoma was reviewed on HR-VW-MR imaging. An intimal flap was defined as a linear layer crossing the arterial lumen that extended to the sidewall. The double lumen sign was

Table 2: Evaluation of aneurysm occlusion status with different imaging modalities

	DSA			κ (95% CI)
	InCO	CO	Total	
TOF-MRA				0.794 (0.579–1.0)
InCO	12	0	12	
CO	3	14	17	
Total	15	14	29	
HR-VW-MR imaging				0.525 (0.255–0.794)
InCO	8	0	8	
CO	7	14	21	
Total	15	14	29	
TOF-MRA combined with HR-VW-MR imaging				0.931 (0.799–1.0)
InCO	14	0	14	
CO	1	14	15	
Total	15	14	29	

Note:—CO indicates complete occlusion; InCO, incomplete occlusion.

defined as 2 lumens represented as 2 jets of flow void within 1 vessel.⁵ An intramural hematoma was identified as a false lumen filled with hematoma.

Statistical Analysis

All statistical analyses were performed in SPSS 26.0 (IBM) and SAS 9.4 (SAS Institute). Quantitative variables are expressed as mean (SD) or median (interquartile range), and qualitative variables are presented as counts (percentages). The aneurysm size is expressed as (the Maximum Diameter Perpendicular to the Parent Artery) \times (the Length of Lesion along the Parent Artery) on preoperative DSA. Interobserver and intermodality consistency were evaluated with κ or weighted κ statistics. The κ value was interpreted as follows:⁹ 0.81–1.00, almost perfect agreement; 0.61–0.80, substantial agreement; 0.41–0.60, moderate agreement; 0.21–0.40, fair agreement; 0.00–0.20, slight agreement; and <0.00 , poor agreement. The Wilcoxon signed-rank test was used to compare image quality between TOF-MRA and HR-VW-MR imaging. With DSA used as the criterion standard to assess the aneurysm occlusion status and parent artery patency, the accuracy, sensitivity, specificity, positive predictive value, and negative predictive value of TOF-MRA, HR-VW-MR imaging, and HR-VW-MR imaging combined with TOF-MRA were calculated. $P < .05$ was considered significant.

RESULTS

Patient and Aneurysm Characteristics

Twenty-seven patients (5 women, 22 men; mean age, 48.7 [SD, 10.3] years; range, 25–66 years) with 29 intracranial VBDA were included in this study. Among those patients, 25 patients had 1 aneurysm, and 2 patients had 2 aneurysms. Twelve (41.4%) aneurysms ruptured before the procedures. The distribution of these aneurysms was as follows: basilar artery, 3 (10.3%); left vertebral artery, 12 (41.4%); right vertebral artery, 13 (44.8%); and vertebrobasilar junction, 1 (3.4%). The average size of these aneurysms was 7.7 (SD, 2.2) \times 13.7 (SD, 5.3) mm. The 29 aneurysms were treated as follows: 24 with stent-assisted coiling (single LVIS, MicroVention, 17; single Enterprise, Codman & Shurtleff, 2; double LVIS, 1; double Enterprise, 2; LVIS + Enterprise, 2), 1 with double

LVIS without coils, 1 with single Tubridge (MicroPort Medical Company) with coiling, 2 with a single Pipeline (Medtronic) alone, and 1 with a double Pipeline without coils. All coils used in this study were bare platinum coils. Seven (24.1%) aneurysms were completely occluded, and 22 (75.9%) aneurysms were incompletely occluded immediately after treatment. The median interval between the procedures and MR imaging examinations was 191 days (range, 49–1128 days; interquartile range, 129–273 days).

Aneurysm Occlusion Status

The assessment of aneurysm occlusion status with different imaging modalities is summarized in Table 2. DSA showed 14 (48.3%) aneurysms with total occlusion and 15 (51.7%) with incomplete occlusion. TOF-MRA and DSA were discordant for 3 (10.3%) aneurysms that showed incomplete occlusion on DSA but were classified as complete occlusion with TOF-MRA ($\kappa = 0.794$). HR-VW-MR imaging and DSA were discordant for 7 (24.1%) aneurysms that showed incomplete occlusion on DSA but were classified as complete occlusion with HR-VW-MR imaging ($\kappa = 0.525$). However, only 1 (3.4%) aneurysm was discordant between HR-VW-MR imaging combined with TOF-MRA and DSA ($\kappa = 0.931$). One aneurysm treated with 2 Pipeline implantations, with small remnants visible on DSA, was classified as complete occlusion on HR-VW-MR imaging combined with TOF-MRA. Figures 1–3 show representative images.

The comparative diagnostic performance of different imaging modalities is shown in Table 3. Whereas TOF-MRA and HR-VW-MR imaging showed a sensitivity and specificity of 80.0% and 100.0% and 53.3% and 100.0%, respectively, HR-VW-MR imaging combined with TOF-MRA showed a sensitivity and specificity of 93.3% and 100.0%, respectively.

Patency of the Parent Artery

The mean image quality score of HR-VW-MR imaging was significantly higher than that of TOF-MRA (4.88 [SD, 0.32] versus 2.53 [SD, 1.25], $P < .001$). Although all HR-VW-MR images had good or excellent image quality (score, ≥ 4), only 31.0% (9/29) of the TOF-MRA images had good or excellent image quality. When the TOF-MRA and HR-VW-MR images were reviewed together, all assessments of the patency of the parent artery were made on the basis of the HR-VW-MR images in this study because the HR-VW-MR imaging provided a better view of the arterial lumen than TOF-MRA in all cases. Four (14.8%) patients showed mild motion artifacts on HR-VW-MR imaging, whereas no motion artifacts were found in TOF-MRA. The motion artifacts were presumed to have been caused by oral motion and had little influence on image quality.

DSA indicated that 25 (86.2%) patients had a normal parent artery, and 4 (13.8%) patients had mild parent artery stenosis ($<50\%$). TOF-MRA indicated that 2 (6.9%) patients had a normal parent artery, 18 (62.1%) patients had parent artery stenosis, and 9 (31.0%) patients had parent artery occlusion. TOF-MRA and DSA were discordant for 23 (79.3%) patients ($\kappa = 0.088$): Nineteen normal parent arteries on DSA were classified as stenosis with TOF-MRA, and 4 other normal parent arteries on DSA were classified as occlusion with TOF-MRA. With the simplified 2-grade scale, the intermodality agreement between DSA and TOF-MRA was 0.023.

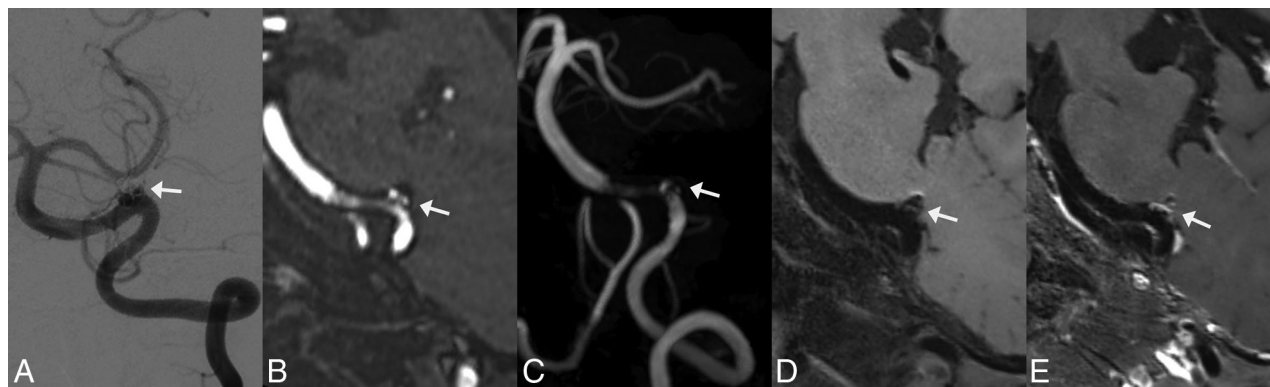


FIG 1. Follow-up images of a left vertebral artery dissecting aneurysm treated by LVIS stent-assisted coiling 6 months after the procedure. *White arrows indicate the location of the aneurysm.* A, DSA shows that the aneurysm involves incomplete occlusion and the stented artery is normal. B and C, MPR and MIP images of TOF-MRA show an aneurysm remnant. Moderate artifacts and a stenosis are observed at the stented artery on TOF-MRA. D and E, On pre- and postcontrast 3D T1-weighted SPACE, though no aneurysm remnant is observed, the stented artery is depicted well and indicates an absence of stenosis. The postcontrast image shows enhancement of the aneurysm wall, aneurysm lumen, and stented artery. The image quality score assigned by the 2 reviewers for TOF-MRA and 3D TIWI SPACE is 3/3 and 5/5, respectively.



FIG 2. Follow-up images of a left vertebral artery dissecting aneurysm treated with LVIS stent-assisted coiling at the third month postoperatively. A, DSA shows recurrence of the aneurysm and mild stenosis of the proximal stented artery. *Arrowheads indicate the stent edges.* B and C, MPR and MIP images of TOF-MRA show the residual aneurysm lumen (*white arrow*) clearly. However, substantial artifacts and severe stenosis are observed at the proximal stented artery on TOF-MRA. D and E, On pre- and postcontrast 3D T1-weighted SPACE, the residual aneurysm lumen (*white arrow*) is depicted clearly, and an intramural hematoma (*outline arrow*) is observed. The depiction of the in-stent lumen is similar to that of DSA, with hardly any artifacts. The postcontrast image shows enhancement of the aneurysm wall, intramural hematoma, and stented artery. The image quality score assigned by the 2 reviewers for TOF-MRA and 3D TIWI SPACE is 2/2 and 5/5, respectively.

The sensitivity, specificity, positive predictive value, negative predictive value, and accuracy of TOF-MRA were 100.0%, 8.0%, 14.8%, 100.0%, and 20.7%, respectively. However, regardless of whether the simplified 2-grade scale or the 3-grade scale was used, the assessment results based on HR-VW-MR imaging were completely consistent with those based on DSA. Therefore, the intermodality agreement was 1.00.

Evaluation of the Vessel Wall

The presence of an intimal flap, double lumen sign, and intramural hematoma (IMH) was observed in 2 (6.9%), 3 (10.3%), and 17 (58.6%) patients, respectively. All intimal flaps and double lumen signs were observed in incompletely occluded aneurysms. Intramural hematomas were observed in 42.9% (6/14) of completely occluded aneurysms and 73.3% (11/15) of incompletely occluded aneurysms, respectively ($P = .139$). Contrast enhancement of the affected vessel wall and intimal flaps was observed in all the cases.

Interobserver Agreement

In the evaluation of the aneurysm occlusion status, the κ value of interobserver agreement for TOF-MRA, HR-VW-MR imaging, HR-VW-MR imaging combined with TOF-MRA, and DSA was 0.86, 0.83, 1.00, and 0.93, respectively.

In the assessment of the patency of the parent artery with the 3-grade scale, the κ value for TOF-MRA, HR-VW-MR imaging, HR-VW-MR imaging combined with TOF-MRA, and DSA was 0.88, 0.84, 0.84, and 0.84, respectively. With the simplified 2-grade scale, the κ value for TOF-MRA, HR-VW-MR imaging, HR-VW-MR imaging combined with TOF-MRA, and DSA was 0.65, 0.84, 0.84, and 0.84, respectively.

DISCUSSION

This study demonstrated that HR-VW-MR imaging combined with TOF-MRA at 3T had high concordance with DSA in the



FIG 3. Follow-up images of a left vertebral artery dissecting aneurysm treated with Enterprise stent-assisted coiling at the sixth month postoperatively. A, DSA shows fusiform dilation (white arrows) of the left vertebral artery. The aneurysm is diagnosed as having incomplete occlusion. Arrowheads indicate the stent edges. B, The MIP image of TOF-MRA shows strong signal loss at the stented artery. The aneurysm remnant is not depicted. C and D, Pre- and postcontrast 3D T1-weighted SPACE shows a fusiform dilation of the parent artery, similar to the DSA findings. The aneurysm is classified as having incomplete occlusion on 3D T1-weighted SPACE. The postcontrast image shows mild enhancement of the stented artery. The image quality score for TOF-MRA and 3D T1-weighted SPACE is 1/1 and 5/5, respectively.

Table 3: Diagnostic performance of TOF-MRA, HR-VW-MR imaging, and HR-VW-MR imaging combined with TOF-MRA in the assessment of aneurysm occlusion status

	Sensitivity	Specificity	Positive Predictive Value	Negative Predictive Value	Accuracy
TOF-MRA	80.0%	100.0%	100.0%	82.4%	89.7%
HR-VW-MR imaging	53.30%	100.0%	100.0%	66.7%	75.9%
HR-VW-MR imaging combined with TOF-MRA	93.3%	100.0%	100.0%	93.3%	96.6%

evaluation of aneurysm occlusion status and the patency of the parent artery in the follow-up of intracranial VBDA after reconstructive EVT. For visualization of the stented artery, HR-VW-MR imaging provided obviously better image quality than TOF-MRA. The interobserver agreement in the image analysis for different imaging modalities ranged from substantial to almost perfect.

Aneurysm Occlusion Status

The aneurysm occlusion status and patency of the parent artery were the 2 major concerns in the follow-up of VBDA. Because TOF-MRA used bright-blood technology to depict the blood flow, the blood flow in the parent artery and residual aneurysm showed high signals, which were distinguishable from those of the surrounding tissues. In contrast, to depict the vessel wall and lumen directly, black-blood technology was used in HR-VW-MR imaging. Because the blood flow signals were suppressed in HR-VW-MR imaging, the residual aneurysm was sometimes difficult to distinguish from surrounding tissues (Fig 1). In general, TOF-MRA was superior to HR-VW-MR imaging in the evaluation of aneurysm occlusion status in our study. However, HR-VW-MR imaging was less sensitive to the susceptibility artifacts caused by stents and coils than TOF-MRA, and the vessel wall features on HR-VW-MR imaging might be helpful in assessing aneurysm occlusion status. Figure 3 shows the follow-up images of a

vertebral artery dissecting aneurysm treated with Enterprise stent-assisted coiling. Whereas the residual aneurysm and most of the stented artery were invisible on TOF-MRA because of artifacts, the HR-VW-MR imaging showed a fusiform dilation of the parent artery, similar to the DSA findings. The aneurysm was classified as incomplete occlusion on DSA and HR-VW-MR imaging. Therefore, the combination of TOF-MRA and HR-VW-MR imaging improved the diagnostic accuracy in the evaluation of aneurysm occlusion status.

In this study, the overall sensitivity and specificity of TOF-MRA in the assessment of aneurysm occlusion status were 80.0% and 100.0%, respectively. Except for 4 aneurysms treated with flow diverters, TOF-MRA had a sensitivity and specificity of 84.6% and 100.0%, respectively, in the rest of the aneurysms treated with stent placement with or without coils. In the largest prospective study on the diagnostic performance of TOF-MRA in the follow-up of treated intracranial aneurysms to date, Xiang et al³ reported a sensitivity and specificity of 0.67 and 0.95, respectively, for aneurysms treated with stent-assisted coiling, and 0.92 and 1.00, respectively, for aneurysms treated with flow diverters. TOF-MRA showed a better diagnostic performance in this study than in previous studies of aneurysms treated with stent placement,^{3,10} possibly because of the use of different treatment concepts for dissecting aneurysms and saccular aneurysms. Because the dissecting aneurysmal wall might be more fragile than the wall of a saccular aneurysm, the

VBDAs may pose greater risk than saccular aneurysms in embolization with coils. The relatively looser coil packing resulted in fewer susceptibility artifacts caused by coils.

Patency of the Parent Artery

The image quality of the stented artery on TOF-MRA was disappointing because TOF-MRA was sensitive to the susceptibility artifacts and radiofrequency shielding artifacts of implanted stents or flow diverters. Consequently, TOF-MRA often showed false stenosis or occlusion of the stented artery (Figs 1 and 3).^{11,12} In contrast, HR-VW-MR imaging showed significantly better image quality than TOF-MRA, with no or few artifacts. This result was consistent with findings from a previous study demonstrating that 3D T1-weighted SPACE was more accurate than TOF-MRA in the assessment of patency of the stented artery in 53 intracranial aneurysms treated with the Pipeline.¹³ In this study, regardless of whether the simplified 2-grade or 3-grade scale was used, the HR-VW-MR imaging had a 100% coincidence rate with DSA in the evaluation of the patency of the parent artery. Therefore, HR-VW-MR imaging is a good technique for assessing the patency of the parent artery in intracranial VBDAs treated with reconstructive EVT.

Evaluation of Vessel Walls

Beyond the aneurysm occlusion status and the patency of the parent artery, attention should also be paid to arterial wall evolution during the follow-up period. In this study, whereas an intimal flap and double lumen sign were observed only in incompletely occluded aneurysms, IMH was observed in both completely occluded and incompletely occluded aneurysms. Complete occlusion of the aneurysms indicated an absence of blood flow into the vessel wall through the ruptured internal elastic lamina but did not indicate that the affected vessel wall was healing well. Tian et al¹⁴ reported that persistent high signal intensity of IMHs may be associated with the progression of intracranial VBDAs after reconstructive EVT. Zhang et al¹⁵ reported 3 VBDAs that were confirmed to have total occlusion on DSA and showed IMH enlargement on MR imaging. Even if the parent arteries are sacrificed, the IMH might continue to enlarge; however, the mechanism is unclear in this circumstance.¹⁵ Some authors have speculated that the rupture of the vasa vasorum in the arterial wall results in IMH recurrence.^{16,17} Therefore, for patients with treated VBDAs whose symptoms persist or worsen, an HR-VW-MR imaging examination is recommended even if the DSA shows that the aneurysms involve total occlusion.

Zhang et al¹⁸ have reported that aneurysm wall enhancement of unruptured VBDAs on HR-VW-MR imaging before procedures might predict an unstable state and can be used to predict aneurysm progression after reconstructive EVT. A study including 53 intracranial saccular aneurysms has reported that aneurysm wall enhancement is commonly observed after embolization and decreases with time.¹⁹ However, no study on affected vessel wall enhancement in VBDAs after reconstructive EVT has been reported. In our study, the affected vessel wall enhancement was observed in all cases. The association between the degree of affected vessel wall enhancement and the stability of VBDAs after reconstructive EVT and the change in vessel wall enhancement with time will be explored in our future studies.

Imaging Protocol

Although HR-VW-MR imaging can be acquired with both 2D and 3D sequences, only the 3D T1-weighted SPACE sequence was performed in this study. The 2D sequences can provide high spatial resolution and a good SNR but require longer acquisition times than 3D sequences when the VBDAs are large.⁴ In contrast, 3D T1-weighted SPACE using isotropic volume scanning can cover a large scope in a relatively short scanning time. In addition, the vessel wall and lumen can be observed from different projections through MPR of 3D SPACE. The major limitation of HR-VW-MR imaging is its relatively long scanning time. The total examination time in our study was nearly 20 minutes. Therefore, the HR-VW-MR imaging examination is not suitable for patients with claustrophobia or postoperative restlessness. To decrease the examination time, we changed the imaging protocol of HR-VW-MR imaging from 2022: First, TOF-MRA was performed to define the location of the vertebrobasilar artery; then, the scanning scope of 3D T1-weighted SPACE was limited to the location of the vertebrobasilar artery. This imaging protocol decreased the examination time by nearly half.

Owing to the high signal intensity of the contrast agent, contrast-enhanced MRA has been reported to be superior to TOF-MRA in the assessment of aneurysmal occlusion status for endovascularly treated intracranial aneurysms.^{11,20} In recent years, Silent MRA (GE Healthcare) and pointwise encoding time reduction with radial acquisition subtraction-based MRA (PETRA; Siemens), both using an arterial spin-labeling combined with an ultrashort TE technique, have been demonstrated to be superior to TOF-MRA in the evaluation of aneurysm occlusion status for endovascularly treated aneurysms.^{10,20-22} Given that most treated intracranial aneurysms in these previous studies were saccular aneurysms, the diagnostic performance of these MRA techniques should be compared in intracranial VBDAs treated with reconstructive EVT in future studies. Because all MRA techniques are unable to provide a precise assessment of the affected arterial wall, HR-VW-MR imaging is always recommended in the follow-up of treated VBDAs.

Limitations

This article had several limitations: First, it was a retrospective study with a small sample size. Second, the exact sizes of dissecting aneurysms should be measured on the 3D SPACE images. Because some patients did not undergo HR-VW-MR imaging before their procedures, the aneurysmal size was measured on the DSA images during their procedures. The exact size of the VBDAs might have been larger because the IMHs could not be visualized on DSA images. Finally, the interval between the procedures and MR examinations varied widely among patients.

CONCLUSIONS

In the follow-up of intracranial VBDAs after reconstructive EVT, HR-VW-MR imaging combined with TOF-MRA at 3T showed good diagnostic performance in the evaluation of aneurysm occlusion status and patency of the parent artery. As a noninvasive imaging technique, the combination of HR-VW-MR imaging and TOF-MRA may be an ideal option for repeat

examinations in patients with intracranial VBDA after reconstructive EVT.

Disclosure forms provided by the authors are available with the full text and PDF of this article at www.ajnr.org.

REFERENCES

1. Sikkema T, Uyttenboogaart M, Eshghi O, et al. Intracranial artery dissection. *Eur J Neurol* 2014;21:820–26 [CrossRef Medline](#)
2. Catapano JS, Ducruet AF, Cadigan MS, et al. Endovascular treatment of vertebral artery dissecting aneurysms: a 20-year institutional experience. *J Neurointerv Surg* 2022;14:257–61 [CrossRef Medline](#)
3. Xiang S, Fan F, Hu P, et al. The sensitivity and specificity of TOF-MRA compared with DSA in the follow-up of treated intracranial aneurysms. *J Neurointerv Surg* 2021;13:1172–79 [CrossRef Medline](#)
4. Sui B, Bai X, Gao P, et al. High-resolution vessel wall magnetic resonance imaging for depicting imaging features of unruptured intracranial vertebrobasilar dissecting aneurysms. *J Int Med Res* 2021;49:30006052097738 [CrossRef Medline](#)
5. Zhu X, Qiu H, Hui FK, et al. Practical value of three-dimensional high resolution magnetic resonance vessel wall imaging in identifying suspicious intracranial vertebrobasilar dissecting aneurysms. *BMC Neurol* 2020;20:199 [CrossRef Medline](#)
6. Wang Y, Lou X, Li Y, et al. Imaging investigation of intracranial arterial dissecting aneurysms by using 3 T high-resolution MRI and DSA: from the interventional neuroradiologists' view. *Acta Neurochir (Wien)* 2014;156:515–25 [CrossRef Medline](#)
7. Wu Y, Wu F, Liu Y, et al. High-resolution magnetic resonance imaging of cervicocranial artery dissection: imaging features associated with stroke. *Stroke* 2019;50:3101–07 [CrossRef Medline](#)
8. Takano N, Suzuki M, Irie R, et al. Usefulness of non-contrast-enhanced MR angiography using a silent scan for follow-up after y-configuration stent-assisted coil embolization for basilar tip aneurysms. *AJNR Am J Neuroradiol* 2017;38:577–81 [CrossRef Medline](#)
9. Landis JR, Koch GG. The measurement of observer agreement for categorical data. *Biometrics* 1977;33:159–74 [CrossRef Medline](#)
10. Kim YN, Choi JW, Lim YC, et al. Usefulness of silent MRA for evaluation of aneurysm after stent-assisted coil embolization. *Korean J Radiol* 2022;23:246–55 [CrossRef Medline](#)
11. Attali J, Benaissa A, Soize S, et al. Follow-up of intracranial aneurysms treated by flow diverter: comparison of three-dimensional time-of-flight MR angiography (3D-TOF-MRA) and contrast-enhanced MR angiography (CE-MRA) sequences with digital subtraction angiography as the gold standard. *J Neurointerv Surg* 2016;8:81–86 [CrossRef Medline](#)
12. Akkaya S, Akca O, Arat A, et al. Usefulness of contrast-enhanced and TOF MR angiography for follow-up after low-profile stent-assisted coil embolization of intracranial aneurysms. *Interv Neuroradiol* 2018;24:655–61 [CrossRef Medline](#)
13. Shao Q, Wu Q, Li Q, et al. Usefulness of 3D T1-SPACE in combination with 3D-TOF MRA for follow-up evaluation of intracranial aneurysms treated with Pipeline embolization devices. *Front Neurol* 2020;11:542493 [CrossRef Medline](#)
14. Tian Z, Chen J, Zhang Y, et al. Quantitative analysis of intracranial vertebrobasilar dissecting aneurysm with intramural hematoma after endovascular treatment using 3-T high-resolution magnetic resonance imaging. *World Neurosurg* 2017;108:236–43 [CrossRef Medline](#)
15. Zhang Y, Wang Y, Sui B, et al. Magnetic resonance imaging follow-up of large or giant vertebrobasilar dissecting aneurysms after total embolization on angiography. *World Neurosurg* 2016;91:218–27 [CrossRef Medline](#)
16. Nakatomi H, Segawa H, Kurata A, et al. Clinicopathological study of intracranial fusiform and dolichoectatic aneurysms: insight on the mechanism of growth. *Stroke* 2000;31:896–900 [CrossRef Medline](#)
17. Ono H, Nakatomi H, Tsutsumi K, et al. Symptomatic recurrence of intracranial arterial dissections: follow-up study of 143 consecutive cases and pathological investigation. *Stroke* 2013;44:126–31 [CrossRef Medline](#)
18. Zhang Y, Sui B, Liu J, et al. Aneurysm wall enhancement on magnetic resonance imaging as a risk factor for progression of unruptured vertebrobasilar dissecting aneurysms after reconstructive endovascular treatment. *J Neurosurg* 2018;128:747–55 [CrossRef Medline](#)
19. Larsen N, Flüh C, Madjidyar J, et al. Visualization of aneurysm healing: enhancement patterns and reperfusion in intracranial aneurysms after embolization on 3T vessel wall MRI. *Clin Neuroradiol* 2020;30:811–15 [CrossRef Medline](#)
20. You SH, Kim B, Yang KS, et al. Ultrashort echo time magnetic resonance angiography in follow-up of intracranial aneurysms treated with endovascular coiling: comparison of time-of-flight, pointwise encoding time reduction with radial acquisition, and contrast-enhanced magnetic resonance angiography. *Neurosurgery* 2021;88:E179–89 [CrossRef Medline](#)
21. Tan S, Lu Y, Li B, et al. Usefulness of silent magnetic resonance angiography in the follow-up of endovascular-treated intracranial aneurysm: a prospective study. *J Stroke Cerebrovasc Dis* 2022;31:106256 [CrossRef Medline](#)
22. Oishi H, Fujii T, Suzuki M, et al. Usefulness of Silent MR angiography for intracranial aneurysms treated with a flow-diverter device. *AJNR Am J Neuroradiol* 2019;40:808–14 [CrossRef Medline](#)